



# Application of thermoresponsive hydrogel/gold nanorods composites in the detection of diquat



Caiyun Jiang<sup>a,b</sup>, Xiaoyuan Ma<sup>c</sup>, Maoyun Xue<sup>b</sup>, Hong-zhen Lian<sup>a,\*</sup>

<sup>a</sup> State Key Laboratory of Analytical Chemistry for Life Science, Collaborative Innovation Center of Chemistry for Life Sciences, School of Chemistry and Chemical Engineering, Nanjing University, Nanjing 210023, China

<sup>b</sup> Jiangsu Engineering and Research Center of Food Safety, Department of Engineering and Technology, Jiangsu Vocational Institute of Commerce, Nanjing 210007, China

<sup>c</sup> State Key Laboratory of Food Science and Technology, School of Food Science and Technology, Jiangnan University, Wuxi 214122, China

## ARTICLE INFO

### Keywords:

N-Isopropylacrylamide  
Gold nanorods  
Diquat  
SERS  
LSPR

## ABSTRACT

Gallic acid (GA) was employed as a reducing agent for facile in situ preparation of gold nanorods (GNRs) in thermoresponsive P(NIPAM-NVP) hydrogel films. Based on the surface-enhanced Raman scattering (SERS) effect of GNRs and the enrichment effect of thermoresponsive hydrogel film on test molecules through a shrinkage process, the obtained P(NIPAM-NVP)/GNRs composites have been used as SERS substrate for the rapid detection of diquat. The influences of substrate pre-treatment, laser wavelength, and sample treatment method on diquat determination have been investigated comprehensively. The results showed the composite material to be a good SERS substrate for highly sensitive detection and a promising preconcentration matrix of diquat. The limit of detection of the proposed protocol was estimated to be  $2.7 \times 10^{-13}$  mol L<sup>-1</sup> for diquat. Notably, diquat could be concentrated with the enrichment factor of about 4 after three times swelling-shrinking processes of the hydrogel film.

## 1. Introduction

Diquat (DQ) is a pyridine-based, broad-spectrum, quick-acting, and nonselective contact herbicide for stem and leaf treatment. Its chemical name is 1,1'-ethylidene-2,2'-bipyridine dibromide monohydrate. Diquat has a rapid effect, especially for broadleaf weeds, and is applicable for the pre-sowing weeding of non-cultivated land and no-tillage farmland as well as inter-row weeding in orchards and crops. Moreover, it can also be used for the withering and disleafing of soybean and cotton before harvest. However, diquat has good stability with a long half-life, and it is toxic to mammals, causing fetal malformation [1].

At present, the common analysis methods for diquat are mainly high-performance liquid chromatography (HPLC) [2] or liquid chromatography-mass spectrometry (LC-MS) [3], capillary electrophoresis (CE) [4], flow injection analysis [5], spectrophotometry [6], electrochemical analysis [7], and fluorescence analysis [8]. However, these methods have some disadvantages, such as time-consuming or complicated sample pre-treatment, long analysis time, which limit the improvement of sensitivity.

Surface-enhanced Raman spectroscopy (SERS) has been widely used in molecular detection due to many advantages, including non-

destruction of samples, rapidity, convenience, and high sensitivity [9,10]. Previous research has indicated that the mechanism of SERS mainly relies on electromagnetic enhancement [11]. If a nano interstitial structure of size less than 10 nm is present between two nanoparticles, the electromagnetic field of the resonance region generated by plasma excitation will be greatly enhanced. Generally, this kind of region is termed a "hot spot". When the molecules to be probed are located in these special hot spots, the enhancement factor in this region can be up to  $10^8$ . The greater the number of hot spots is, the greater the enhancement effect is. In recent years, with considerable progress in the controllable preparation of SERS substrates, SERS technology has been increasingly applied in quantitative determination and trace analysis. Gold nanorods (GNRs) have a very strong Raman enhancing effect [12]. Moreover, the localized surface plasma resonance (LSPR) frequency can be adjusted by controlling the length/diameter ratio of the rods to match the frequency of Raman excitation light, thus realizing the optimal enhancement effect [13]. N-Isopropylacrylamide (NIPAM) hydrogel is an "intelligent" thermoresponsive material. It exhibits adjustable chemical properties, three-dimensional physical structure, excellent mechanical properties, high water content, and good biocompatibility, and has been widely used in separation, catalysis, and biological and medical fields [14].

\* Corresponding author.

E-mail address: [hzlian@nju.edu.cn](mailto:hzlian@nju.edu.cn) (H.-z. Lian).

In this study, gallic acid (GA) has been innovatively used instead of ascorbic acid (AA) in the conventional preparation process of GNRs. The equilibrium between diffusion rate and reaction rate was adjusted using GA as the reducing agent. The GNRs were simply prepared in situ in P(NIPAM-NVP) thermoresponsive hydrogel films. The resulting P(NIPAM-NVP)/GNRs composites have been applied in the SERS detection of diquat, exploiting the Raman enhancement effect of the GNRs. The distance between the GNPs could be adjusted through the shrinking behavior of the hydrogel to generate a better SERS enhancement effect, allowing for rapid and highly sensitive detection of diquat molecules. On the other hand, diquat molecules could be captured and enriched based on the network structure and swelling-shrinking property of the P(NIPAM-NVP) hydrogel films, making the further improvement of detection sensitivity for the analyst.

## 2. Materials and methods

### 2.1. Preparation of P(NIPAM-NVP) hydrogel films

P(NIPAM-NVP) hydrogel films were prepared by a previously reported method with minor modification [15]. In brief, the mixture solution containing NIPAM (0.2 g, high-purity reagent, Tokyo Chemical Industry), N-vinyl-2-pyrrolidone (NVP, 20  $\mu\text{L}$ , high-purity reagent, Tokyo Chemical Industry), ammonium peroxydisulfate (APS, 40  $\mu\text{L}$ , 0.042 mol L<sup>-1</sup>, Sinopharm Chemical Reagent Co., Ltd.), N,N-methylenebisacrylamide (BIS, 290  $\mu\text{L}$ , 25 mg mL<sup>-1</sup>, Sinopharm Chemical Reagent Co., Ltd.) and N,N,N',N'-tetramethylethylenediamine (TEMED, 1  $\mu\text{L}$ , Sinopharm Chemical Reagent Co., Ltd.) was injected into a mold (the thickness of the holding strip was about 0.14 mm), which was then kept in darkness at 4 °C for 12 h until a hydrogel was formed. The hydrogel film was cut into uniform circular slices (diameter ca. 1 cm) with a puncher. The prepared slices were purified by dialysis to remove the cross-linkers and unreacted monomers.

### 2.2. Preparation of P(NIPAM-NVP)/seeds

A 0.2 mol L<sup>-1</sup> aqueous solution of cetyltrimethylammonium bromide (CTAB, 5 mL, Sinopharm Chemical Reagent Co., Ltd.) was placed in a 25-mL beaker. A 5  $\times 10^{-4}$  mol L<sup>-1</sup> aqueous solution of tetrachloroauric acid (HAuCl<sub>4</sub>, 5 mL, Sinopharm Chemical Reagent Co., Ltd.) was added with stirring. After homogeneous dispersion, several pieces of hydrogel films were added and the mixture was left to stand for 5 min. A freshly prepared 0.01 mol L<sup>-1</sup> solution of sodium borohydride (NaBH<sub>4</sub>, 0.6 mL, Sinopharm Chemical Reagent Co., Ltd.) at 0 °C was then added to the solution in one portion. The solution changed from light yellow to brown yellow, and the P(NIPAM-NVP)/seeds hydrogel films were stored at 25 °C for 15 min prior to use.

### 2.3. Preparation of P(NIPAM-NVP)/GNRs

The growth solution was prepared which contained 1 mL of HAuCl<sub>4</sub> (1  $\times 10^{-3}$  mol L<sup>-1</sup>), 1 mL of CTAB (0.2 mol L<sup>-1</sup>) and 50  $\mu\text{L}$  of AgNO<sub>3</sub> (4  $\times 10^{-4}$  mol L<sup>-1</sup>, Sinopharm Chemical Reagent Co., Ltd.). Then, 30  $\mu\text{L}$  of GA (0.0788 mol L<sup>-1</sup>, Sinopharm Chemical Reagent Co., Ltd.) was added into the growth solution. When the solution changed from dark brown yellow to colorless, a piece of P(NIPAM-NVP)/seeds film was taken out from the above brown yellow solution, washed with ultra-pure water, and then put into the above growth solution and reacted for 3 h.

### 2.4. Preparation of GNRs

In order to compare the influence of different reducing agents on the preparation of GNRs, GA and AA (Sinopharm Chemical Reagent Co., Ltd.) were used as reducing agents to prepare GNRs after gold seeds were pre-synthesized. GNRs were prepared by a previously

reported method with minor modification [16]. In briefly, 5 mL of 0.2 mol L<sup>-1</sup> CTAB solution and 5 mL of 5  $\times 10^{-4}$  mol L<sup>-1</sup> HAuCl<sub>4</sub> solution were placed in a beaker with stirring. Then, 0.6 mL of freshly prepared NaBH<sub>4</sub> solution (0.01 mol L<sup>-1</sup>) at 0 °C was mixed rapidly. After further stirring for 2 min, the prepared solution was stored at 25 °C for 2 h. 2.5 mL of HAuCl<sub>4</sub> solution (1  $\times 10^{-3}$  mol L<sup>-1</sup>), 2.5 mL of CTAB solution (0.2 mol L<sup>-1</sup>) and 125  $\mu\text{L}$  of AgNO<sub>3</sub> solution (4  $\times 10^{-3}$  mol L<sup>-1</sup>) were mixed with stirring in another beaker. Then, a 0.0078 mol L<sup>-1</sup> GA or AA aqueous solution (90  $\mu\text{L}$ ) was added. When the color of the solution changed from dark brown yellow to pale yellow, 25  $\mu\text{L}$  of gold seeds solution were added for subsequent reaction at 27 °C.

### 2.5. Characterization of P(NIPAM-NVP)/GNRs

The optical properties of as-prepared P(NIPAM-NVP)/GNRs, as well as the GNRs for comparison study were characterized by means of a spectrophotometer (UV-3150, Shimadzu Corporation, Japan) with a temperature control device. The morphology of the GNRs was observed by a transmission electron microscope (JEM-2100EX, JEOL Corporation, Japan). The X-ray diffraction (XRD) pattern of P(NIPAM-NVP)/GNRs was collected on an X-ray diffractometer (Rigaku Corporation, Japan) using Cu K $\alpha$  radiation operated at 40 kV and 200 mA to characterize the crystallographic phases of GNRs in the hydrogels. For SERS determination, a P(NIPAM-NVP)/GNRs film was immersed in diquat solution and the residual solution on its surface was rinsed off with ultra-pure water. The P(NIPAM-NVP)/GNRs film was laid on the surface of a glass slide, and the molecular signal was measured by means of a Raman spectrometer (Renishaw Invia Reflex, Renishaw Corporation, England).

## 3. Results and discussion

### 3.1. Preparation of P(NIPAM-NVP)/GNRs composites

Research on the preparation process of P(NIPAM-NVP)/GNRs composites has indicated that an appropriate equilibrium relationship between diffusion rate and reaction rate is very important for the preparation of GNRs in a hydrogel network [15]. The reduction rate of the reducing agent (i.e., AA) may be slowed down by decreasing the pH of the reaction solution, which is advantageous to the equilibrium between diffusion rate and reaction rate within and outside of the hydrogel. Thus, the formation of GNRs in the hydrogel is rendered controllable. According to the conventional preparation method of GNRs, an acid medium is required to reduce the reduction rate of AA, such that equilibrium is established between diffusion rate and reaction rate. In this study, GA has been selected as a reducing agent, which significantly reduces the reaction rate even not lowering pH with an acid. Fig. 1 shows the relationship between spectral change and reaction time during the growth process of GNRs. It can be seen that the reduction rate of AA was relatively fast, and the reaction was complete within 10 min. However, the reaction endpoint was only reached after 50 min for GA. Therefore, the reaction was moderated and hence more easily controlled when GA was used as a reducing agent. As a general preparation method, the mechanism for the formation of GNRs in AA system has been elucidated extensively [16]. In this study, GA has been used for the first time in the facile synthesis of GNRs. The formation mechanism is explained that it is likely related to the structure of polyphenols in GA. Theoretical and experimental investigations have revealed that polyphenolic compounds such as GA and their derivatives are known to form complexes with metal cations and their ability to chelate metal ions is a more probable mode of action than their oxidation process [17,18]. In GA system, the complex reaction of gold ions with the phenolic hydroxyl groups might occur, leading to significant decrease of the reaction rate. Therefore, the reaction was moderated and hence easily controlled when GA was used as a reducing agent.

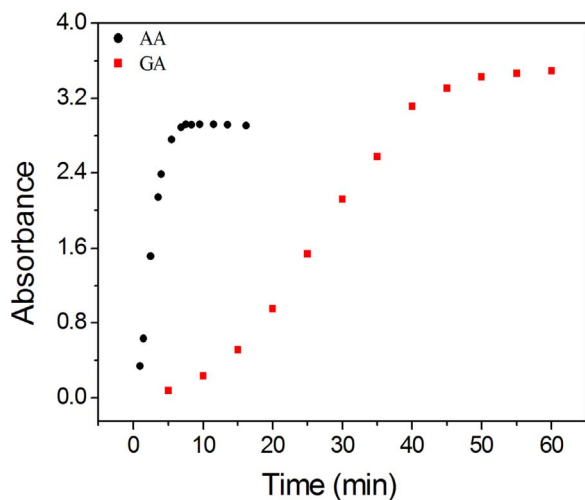


Fig. 1. Influence of reducing agent on the growth time of GNRs.

Fig. 2 shows the TEM image of a P(NIPAM-NVP)/GNRs composite film prepared using GA. In order to investigate the morphology of GNRs in the hydrogel film, the film was subjected to a sequence of resin embedding, cutting, and TEM observation. It was found that GNRs were distributed in the film. The morphology was relatively uniform. Some particles with irregular morphology were seen in the image, which can be mainly attributed to differences in the position and cutting angle of the GNRs. As shown in Fig. S1, XRD peaks from atomic lattices of the GNRs emerged at  $2\theta=38.2^\circ$ ,  $44.5^\circ$ ,  $64.3^\circ$  and  $77.6^\circ$ , and because these peaks are consistent with JCPDS 04–0784, they are assigned to (111), (200), (220) and (311) reflection lines, respectively. The XRD pattern showed primarily the (111) Bragg reflection of face-centered cubic (FCC)-structured gold crystals, whereas the (200), (220) and (311) Bragg reflections were extremely weak, indicating highly oriented growth of the GNRs. This is powerful evidence of the preferential growth of the GNRs in the hydrogel film along the (111) direction as the particle length increases.

### 3.2. Thermoresponsive-SERS properties of P(NIPAM-NVP)/GNRs

Fig. 3 shows the SERS spectrum of a diquat solution ( $10^{-6}$  mol L $^{-1}$ ) obtained using P(NIPAM-NVP)/GNRs as the substrate and the direct

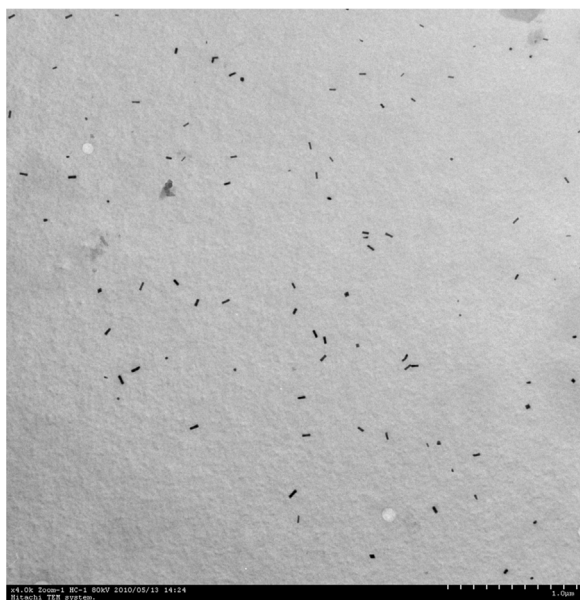


Fig. 2. Cross-sectional TEM image of the P(NIPAM-NVP)/GNRs.

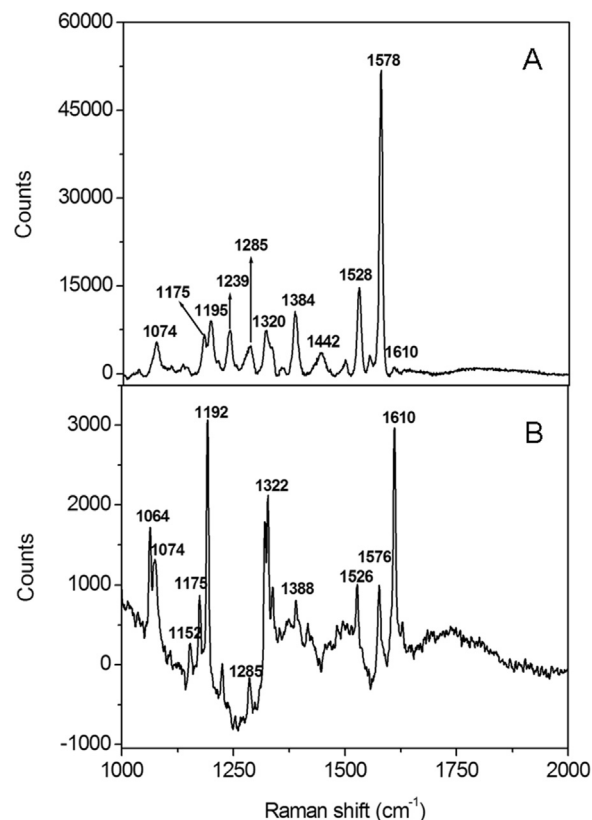
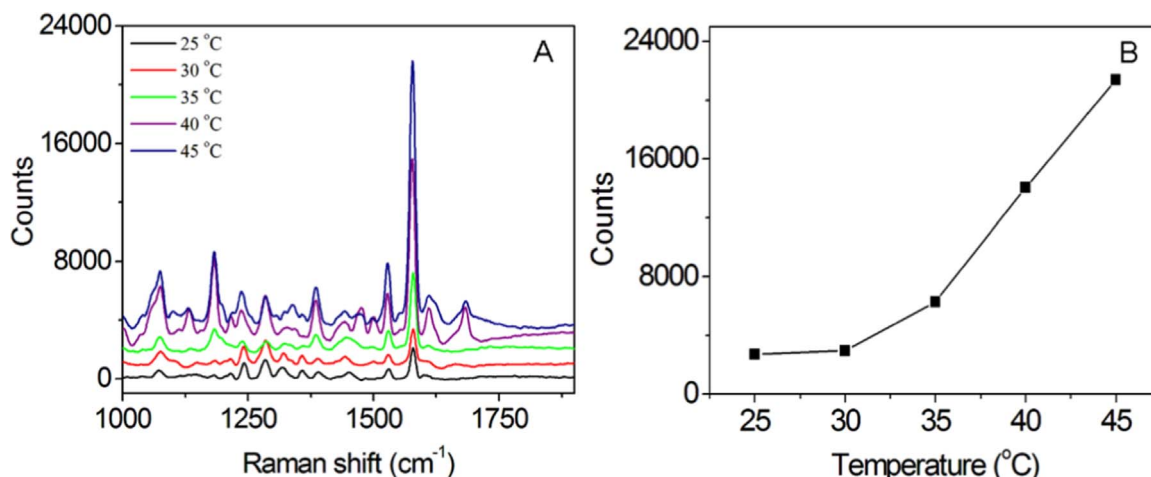


Fig. 3. A. SERS spectrum of diquat in solution ( $10^{-6}$  mol L $^{-1}$ ); B. Raman spectrum of diquat in the solid state.

Raman spectrum of diquat powder. It can be seen that both conditions gave good spectral resolution. However, the SERS spectral intensity of the diquat solution was stronger than that of the solid powder, indicating that the substrate provided a good enhancement effect [19,20]. The relative intensities of some of the peaks in the respective spectra were different. The peaks at  $\nu=1384$ ,  $1528$  and  $1578$  cm $^{-1}$  in the SERS spectrum were significantly enhanced. These peaks were also discernible in the Raman spectrum of solid diquat, but their intensities were comparatively weak. The enhancement of peak intensity could be attributed to the mutual interaction between GNRs and the dipyriddy structure of diquat molecule. Hence, the intensities in the SERS spectrum were different from those in the Raman spectrum of the solid sample. In particular, the peak at  $\nu=1442$  cm $^{-1}$  was obviously enhanced, whereas it was barely detectable in the Raman spectrum of solid diquat. It corresponded to the C–H bending vibration, which further proved the excellent SERS enhancement effect of P(NIPAM-NVP)/GNRs on diquat.

Fig. 4 shows the variation in the SERS spectra of diquat at different temperatures. It can be seen that the SERS signals of diquat were significantly enhanced with increasing temperature and shrinkage of the hydrogel film. The characteristic peak at  $\nu=1578$  cm $^{-1}$  was selected for a comparative study. According to formula (1) [21], the enhancement factor (EF) at  $45^\circ\text{C}$  was 8 times higher than that at  $25^\circ\text{C}$ . The higher the density of GNRs in the hydrogel was, the more obvious the influence of temperature was on the SERS effect. Shrinkage of the hydrogel film caused by an increase in temperature influenced two aspects [22]. Firstly, the refractive index of the medium around the GNRs increased, and based on relevant research results, this would enhance the SERS intensity. Secondly, the number of GNRs per unit area of the spots increased, which increased the number of molecules to be detected, thereby enhancing the SERS intensity.

$$EF = (I_{SERS}/N_{surf}) \times (I_{Raman}/N_{bulk}) \quad (1)$$



**Fig. 4.** A. SERS spectra of diquat on P(NIPAM-NVP)/GNRs substrates at different temperatures from 25 to 45 °C; B. the corresponding relationship between the SERS intensity at 1578 cm<sup>-1</sup> and temperature.

Here,  $I_{SERS}$  and  $I_{Raman}$  are the intensities in the SERS and Raman spectra, respectively,  $N_{bulk}$  is the number of probe molecules without using an enhancing substrate, and  $N_{surf}$  is the number of probe molecules adsorbed on the surface of GNRs as a substrate. Since the Raman spectrum of solid diquat could be directly measured without a solvent, its concentration in this case could be considered as 100%. The diquat concentration for SERS was 10<sup>-6</sup> mol L<sup>-1</sup>.

### 3.3. Pre-treatment of SERS substrate

The main reason for SERS is enhancement of the electromagnetic field. The distribution of an electromagnetic field is closely related to the morphology and position of metal nanoparticles. The electromagnetic field is stronger at a surface where metal nanoparticles are closer to each other. Therefore, the most important factor in actual SERS application is the distance between test molecule and SERS substrate. Under otherwise identical conditions, the smaller the distance was, the higher the SERS intensity was [23,24]. In this study, the GNRs were prepared in situ, rather than incorporated into the hydrogel film after polymerization. This obviated the need for modification of the GNRs and prevented interference from modifiers or stabilizers [25]. However, CTAB was inevitably used in the preparation of the GNRs. Much CTAB was adsorbed on the surfaces of the GNRs, which had two disadvantages: (1) the molecules to be tested could not get close to the surfaces of the GNRs; (2) the positive charges on CTAB would hinder the adsorption of dipyrindyl cations. Therefore, CTAB on the surface of the GNRs should be removed as much as possible. We washed P(NIPAM-NVP)/GNRs with repeated heating and cooling cycles. The results in Fig. 5 proved that the SERS spectrum of diquat was significantly enhanced when washed P(NIPAM-NVP)/GNRs was used as the substrate.

### 3.4. Selection of laser wavelength

It can be clearly seen from Fig. 6 that the SERS signal of diquat increased in intensity when the excitation laser wavelength was increased from 532 to 785 nm. There was no signal at 532 nm. Only the signal at  $\nu=1578$  cm<sup>-1</sup> could be discerned at 633 nm, whereas the SERS signal was greatly enhanced at 785 nm. Almost all the characteristic peaks of diquat were resolved at 785 nm, which could be attributed to the improvement in matching between the strong longitudinal LSPR peaks of the GNRs and the laser excitation wavelength [26,27]. It is well known that the surface plasma is substantially a light wave captured on the surface due to the interaction with free electrons on the conductor surface. The incident light compels the free electrons on the conductor surface to vibrate collectively. When the collective

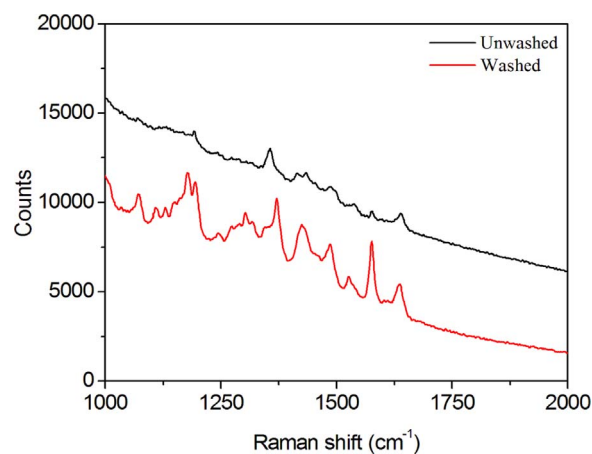


**Fig. 5.** SERS spectra of diquat using unwashed and washed P(NIPAM-NVP)/GNRs as substrates.

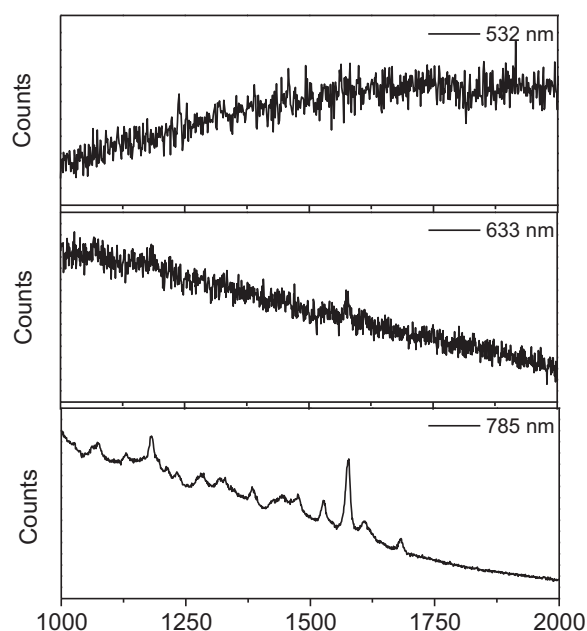


**Fig. 6.** SERS spectra of diquat at different excitation laser wavelengths.

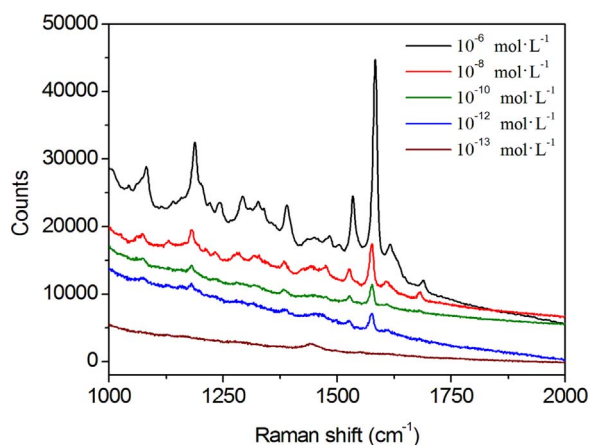


Fig. 7. SERS spectra of diquat at different concentrations.

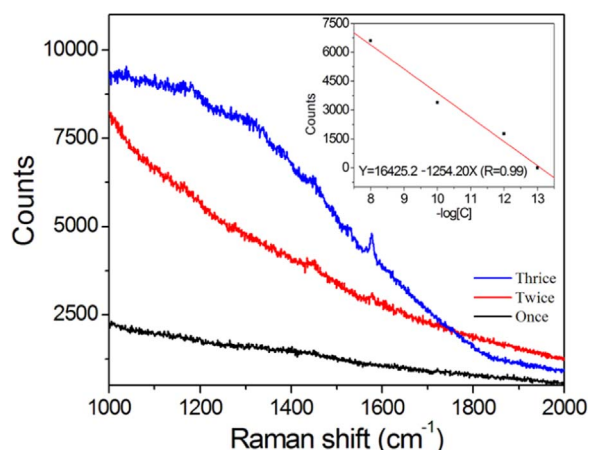


Fig. 8. Enrichment of  $10^{-13}$  mol  $L^{-1}$  diquat by the P(NIPAM-NVP)/GNRs. Inset illustrates the linear correlation of SERS values versus the concentrations of diquat over the range  $10^{-8}$ – $10^{-12}$  mol  $L^{-1}$ .

vibrational frequency is consistent with the frequency of the incident light, resonance occurs. Meanwhile, the electromagnetic field is greatly enhanced, leading to a pronounced surface plasma enhancement effect [28]. It has been found that both LSPR and SERS have strong nano-size dependences, indicating a close relationship between them. The relationship between LSPR and SERS is a subject of much ongoing research. Dieringer et al. developed a kind of wavelength-scanning, surface-enhancing Raman excitation spectrometer. Their experimental results showed that the maximum SERS enhancement is obtained when the LSPR maximum wavelength of the substrate is between the excitation and vibration wavelengths [29], which are supported by the present study.

### 3.5. Limit of detection (LOD)

Diquat solutions of various concentrations were determined to assess the detection sensitivity using P(NIPAM-NVP)/GNRs as a SERS substrate. It can be seen from Fig. 7 that the intensity of the characteristic peak at  $\nu=1578$   $cm^{-1}$  decreased with decreasing diquat concentration. Nevertheless, the characteristic peak could still be clearly detected when the diquat concentration was decreased to  $10^{-12}$  mol  $L^{-1}$ . The LOD was  $2.7 \times 10^{-13}$  mol  $L^{-1}$  which corresponded to the signal equivalent to about three times of noise (3 S/N). Compared to other conventional methods [30,31], the proposed method exhibited lower detection limit, easier operation and shorter analysis time, making it a sensitive and rapid determination method for diquat.

### 3.6. Enrichment performance

Pre-shrunk P(NIPAM-NVP)/GNRs was placed in a diquat solution of concentration  $10^{-13}$  mol  $L^{-1}$  and taken out when it was swollen. The SERS spectrum was measured after air drying. The sample was then re-immersed in the diquat solution ( $10^{-13}$  mol  $L^{-1}$ ) and taken out when it was swollen. The SERS spectrum was measured again after air drying. The operation was repeated several times. The result in Fig. 8 shows that the characteristic peak of diquat gradually increased with increasing number of swelling–shrinking processes. After three operations, the signal intensity of diquat increased around 4 times, indicating a good enrichment effect of this analyte on P(NIPAM-NVP)/GNRs. Good contact between the test molecules and substrate is an important factor for obtaining desired SERS signals. The P(NIPAM-NVP) hydrogel film possessed excellent volume shrinking–swelling properties. Starting from the shrunken hydrogel, the internal negative pressure generated during its swelling process would force the sample solution to enter its network structure.

## 4. Conclusion

GA has been used as a novel reducing agent to easily prepare GNRs in situ in P(NIPAM-NVP) hydrogel films. The resulting P(NIPAM-NVP)/GNRs composites have been used as a SERS substrate to determine diquat. The capture and concentration of diquat molecules were realized by the network structure and swelling–shrinking property of P(NIPAM-NVP) hydrogel, and detection was aided by the Raman enhancement effect of the GNRs. The influences of substrate pre-treatment and laser wavelength on the analytical performance have been investigated in detail. The LOD of this method was estimated as  $2.7 \times 10^{-13}$  mol  $L^{-1}$ . Diquat could thus be rapidly and sensitively detected with the enrichment factor of about 4 after three times swelling–shrinking processes of the hydrogel film.

## Acknowledgments

This work was supported by the National Natural Science Foundation of China (31401665, 21577057 and 91643105); the Natural Science Foundation of Jiangsu Province (BK20161479); the Research of Natural Science in Colleges and Universities in Jiangsu Province (16KJB150043); Qing Lan Project of Jiangsu Province (2016001), the Innovative Training Program for College Students in Jiangsu Province and the Important Projects of Jiangsu Vocational Institute of Commerce (JSJM15005).

## Appendix A. Supporting information

Supplementary data associated with this article can be found in the online version at doi:10.1016/j.talanta.2017.06.010.

## References

- [1] G.M. Jones, J.A. Vale, Mechanisms of toxicity, clinical features, and management of diquat poisoning: a review, *J. Toxicol. Clin. Toxicol.* 38 (2000) 123–128.
- [2] S. Hara, N. Sasaki, D. Takase, S. Shiotsuka, K. Ogata, K. Futagami, K. Tamura, Rapid and sensitive HPLC method for the simultaneous determination of paraquat and diquat in human serum, *Anal. Sci.* 23 (2007) 523–531.
- [3] X.P. Lee, T. Kumazawa, M. Fujishiro, C. Hasegawa, T. Arinobu, H. Seno, A. Ishii, K. Sato, Determination of paraquat and diquat in human body fluids by high-performance liquid chromatography/tandem mass spectrometry, *J. Mass Spectrom.* 39 (2004) 1147–1152.
- [4] Q.X. Zhou, J.L. Mao, J.P. Xiao, G.H. Xie, Determination of paraquat and diquat preconcentrated with N doped TiO<sub>2</sub> nanotubes solid phase extraction cartridge prior to capillary electrophoresis, *Anal. Methods* 2 (2010) 1063–1068.
- [5] T. Perezruiz, C. Martinezlozano, V. Tomas, Simultaneous flow-injection determination of diquat and paraquat in foodstuffs, natural-waters and biological-fluids, *Int. J. Environ. Anal. Chem.* 44 (1991) 243–252.
- [6] S. Tunc, O. Duman, I. Soylu, B.K. Bozoglan, Study on the bindings of dichloroprop and diquat dibromide herbicides to human serum albumin by spectroscopic methods, *J. Hazard. Mater.* 273 (2014) 36–43.

- [7] D.S. De, S.A.S. Machado, Study of the electrochemical behavior and sensitive detection of pesticides using microelectrodes allied to square-wave voltammetry, *Electroanalysis* 18 (2006) 862–872.
- [8] G.X. Song, Q. Tang, Y. Huang, R.B. Wang, Y.Y. Xi, X.L. Ni, Z. Tao, S.F. Xue, J.X. Zhang, A host-guest complexation based fluorescent probe for the detection of paraquat and diquat herbicides in aqueous solutions, *RSC Adv.* 5 (2015) 100316–100321.
- [9] S.H. Seo, B.M. Kim, A. Joe, H.W. Han, X.Y. Chen, Z. Cheng, E.S. Jiang, NIR-light-induced surface-enhanced Raman scattering for detection and photothermal/photodynamic therapy of cancer cell using methylene blue-embedded gold nanorod@SiO<sub>2</sub> nanocomposites, *Biomaterials* 35 (2014) 3309–3318.
- [10] L.L. Zhang, C.L. Jiang, Z.P. Zhang, Graphene oxide embedded sandwich nanostructures for enhanced Raman readout and their applications in pesticide monitoring, *Nanoscales* 5 (2013) 3773–3779.
- [11] X.M. Qian, X. Zhou, S.M. Nie, Surface-enhanced Raman nanoparticle beacons based on bioconjugated gold nanocrystals and long range plasmonic coupling, *J. Am. Chem. Soc.* 130 (2008) 14934–14935.
- [12] J.J. Li, H.Q. An, J. Zhu, J.W. Zhao, Improve the surface enhanced Raman scattering of gold nanorods decorated graphene oxide: the effect of CTAB on the electronic transition, *Appl. Surf. Sci.* 347 (2015) 856–860.
- [13] R. Boyack, E.C. Le Ru, Investigation of particle shape and size effects in SERS using T-matrix calculations, *Phys. Chem. Chem. Phys.* 11 (2009) 7398–7405.
- [14] I. Tokarev, S. Minko, Stimuli-responsive hydrogel thin films, *Soft Matter* 5 (2009) 511–524.
- [15] C.Y. Jiang, Y. Qian, Q. Gao, J. Dong, W.P. Qian, In situ controllable preparation of gold nanorods in thermo-responsive hydrogels and their application in surface-enhanced Raman scattering, *J. Mater. Chem.* 20 (2010) 8711–8716.
- [16] B. Nikoobakht, M.A. El-Sayed, Preparation and growth mechanism of gold nanorods (NRs) using seed-mediated growth method, *Chem. Mater.* 15 (2003) 1957–1962.
- [17] K. Yoosaf, B.I. Ipe, C.H. Suresh, K.G. Thomas, In situ synthesis of metal nanoparticles and selective naked-eye detection of lead ions from aqueous media, *J. Phys. Chem. C* 111 (2007) 12839–12847.
- [18] J. Moilanen, M. Karonen, P. Tähtinen, R. Jacquet, S. Quideau, J.P. Salminen, Biological activity of ellagitannins: effects as anti-oxidants, pro-oxidants and metal chelators, *Phytochemistry* 125 (2016) 65–72.
- [19] M.R. Lopez-Ramirez, L. Guerrini, J.V. Garcia-Ramos, S. Sanchez-Cortes, Vibrational analysis of herbicide diquat: a normal Raman and SERS study on Ag nanoparticles, *Vib. Spectrosc.* 48 (2008) 58–64.
- [20] Z.Y. Wang, X.Q. Ma, S.F. Zong, Y.Z. Wang, H. Chen, Y.P. Cui, Preparation of a magnetofluorescent nano-thermometer and its targeted temperature sensing applications in living cells, *Talanta* 131 (2015) 259–265.
- [21] H. Chew, D.D. Cooke, M. Kerker, Raman and fluorescent scattering by molecules embedded in dielectric cylinders, *Appl. Opt.* 19 (1980) 44–52.
- [22] H. Yockell-Lelievre, F. Lussier, J.F. Masson, Influence of the particle shape and density of self-assembled gold nanoparticle sensors on LSPR and SERS, *J. Phys. Chem. C* 119 (2015) 28577–28585.
- [23] A.D. McFarland, M.A. Young, J.A. Dieringer, R.P. Van Duyne, Wavelength-scanned surface-enhanced Raman excitation spectroscopy, *J. Phys. Chem. B* 109 (2005) 11279–11285.
- [24] A.C. Manikas, A. Aliberti, F. Causa, E. Battista, P.A. Netti, Thermoresponsive PNIPAAm hydrogel scaffolds with encapsulated AuNPs show high analyte-trapping ability and tailored plasmonic properties for high sensing efficiency, *J. Mater. Chem. B* 3 (2015) 53–58.
- [25] K.L. Norrod, K.L. Rowlen, Ozone-induced oxidation of self-assembled decanethiol: contributing mechanism for "photooxidation", *J. Am. Chem. Soc.* 120 (1998) 2656–2657.
- [26] C.E. Taylor, S.D. Garvey, J.E. Pemberton, Carbon contamination at silver surfaces: surface preparation procedures evaluated by Raman spectroscopy and X-ray photoelectron spectroscopy, *Anal. Chem.* 68 (1996) 2401–2408.
- [27] J.M. Chalmers, P.R. Griffiths, *Handbook of Vibrational Spectroscopy*, Wiley, New York, 2002, pp. 759–774.
- [28] T.R. Jensen, M.D. Malinsky, C.L. Haynes, R.P. Van Duyne, Nanosphere lithography: tunable localized surface plasmon resonance spectra of silver nanoparticles, *J. Phys. Chem. B* 104 (2000) 10549–10556.
- [29] T. Vo-Dinh, F. Yan, D.L. Stokes, Plasmonics-based nanostructures for surface-enhanced Raman scattering bioanalysis, *Methods Mol. Biol.* 300 (2005) 255–283.
- [30] T.G. Diaz, I.D. Meras, M.F.A. Franco, Stopped flow kinetic-spectrophotometric determination of diquat in waters, *Water Res.* 36 (2002) 783–787.
- [31] D.J. Barker, R.P. Cooney, L.A. Summers, Resonance Raman spectra of radical cations of bridged diquatery salts of 2,2'-bipyridine, *J. Raman Spectrosc.* 16 (1985) 265–271.